

Highpressure phases of NaAlH₄ from first principles

XiangFeng Zhou, Xiao Dong, Zhisheng Zhao, Artem R. Oganov, Yongjun Tian et al.

Citation: *Appl. Phys. Lett.* **100**, 061905 (2012); doi: 10.1063/1.3682317

View online: <http://dx.doi.org/10.1063/1.3682317>

View Table of Contents: <http://apl.aip.org/resource/1/APPLAB/v100/i6>

Published by the [American Institute of Physics](#).

Related Articles

Influence of monovalent ions on density fluctuations in hydrothermal aqueous solutions by small angle X-ray scattering

J. Chem. Phys. **136**, 044515 (2012)

Nanoscale diffraction imaging of the high-pressure transition in Fe_{1-x}O

Appl. Phys. Lett. **100**, 041903 (2012)

High-pressure study of tetramethylsilane by Raman spectroscopy

J. Chem. Phys. **136**, 024503 (2012)

High-pressure optical and vibrational properties of CdGa₂Se₄: Order-disorder processes in adamantine compounds

J. Appl. Phys. **111**, 013518 (2012)

High pressure transport, structural, and first principles investigations on the fluorite structured intermetallic, PtAl₂

J. Appl. Phys. **111**, 013507 (2012)

Additional information on *Appl. Phys. Lett.*

Journal Homepage: <http://apl.aip.org/>

Journal Information: http://apl.aip.org/about/about_the_journal

Top downloads: http://apl.aip.org/features/most_downloaded

Information for Authors: <http://apl.aip.org/authors>

ADVERTISEMENT



LakeShore Model 8404 developed with **TOYO Corporation**
NEW AC/DC Hall Effect System Measure mobilities down to 0.001 cm²/V s

High-pressure phases of NaAlH₄ from first principles

Xiang-Feng Zhou (周向锋),¹ Xiao Dong (董校),¹ Zhisheng Zhao (赵智胜),² Artem R. Oganov,^{3,4} Yongjun Tian (田永君),² and Hui-Tian Wang (王慧田)^{1,5,a)}

¹Key Laboratory of Weak-Light Nonlinear Photonics and School of Physics, Nankai University, Tianjin 300071, China

²State Key Laboratory of Metastable Materials Science and Technology, Yanshan University, Qinhuangdao 066004, China

³Department of Geosciences and Department of Physics and Astronomy, New York Center for Computational Sciences, Stony Brook University, Stony Brook, New York 11794-2100, USA

⁴Department of Geology, Moscow State University, 119992 Moscow, Russia

⁵National Laboratory of Solid State Microstructures, Nanjing University, Nanjing 210093, China

(Received 17 November 2011; accepted 17 January 2012; published online 8 February 2012)

High-pressure phases of NaAlH₄ are predicted using the *ab initio* evolutionary algorithm. Our first-principles calculations reveal that the low-pressure I4_{1/a} phase containing AlH₄ tetrahedra transforms into the monoclinic P2_{1/c} phase at 3.8 GPa and then into the orthorhombic Ima2 phase at 20.5 GPa. The predicted two structures contain AlH₆ octahedra and AlH₇ decahedra, respectively. Coexistence of P2_{1/c} and Ima2 phases can explain better the measured x-ray diffraction patterns, transition pressure, and volume contraction. Our results provide a comprehensive understanding for the experimental findings. © 2012 American Institute of Physics. [doi:10.1063/1.3682317]

Sodium alanate, NaAlH₄, belongs to the class of complex metal hydrides, which have attracted special interest due to the relatively high hydrogen-storage capacity and the ready reversibility with the aid of transition metal dopants.^{1,2} Hence, NaAlH₄ has been extensively studied as a template for developing hydrogen-storage solutions.^{3–6} An alternative method to improve the reversible hydrogen absorption or desorption kinetics is to search for possibility to stabilize the high-pressure phase of NaAlH₄ at ambient pressure by the appropriate treatments.^{7–11} NaAlH₄ exists at atmospheric pressure in a tetragonal structure. It has been predicted to undergo a structural transition from the tetragonal I4_{1/a} structure (α phase) to the orthorhombic Cmc2₁ structure (β phase) at the pressure of 6.4 GPa with a 4% volume contraction.⁷ Talyzin and Sundqvist performed high pressure Raman experiments up to 17 GPa and found two possible phase transitions: one at \sim 3 GPa, which is less obvious as a structural transformation and another at \sim 14 GPa to an orthorhombic structure.⁹ These results were also further confirmed by the experiments done at up to 27 GPa in Ref. 10. Very interestingly, no phase transition at \sim 3 GPa was found in the measurement of Ref. 10, in which the proposed high-pressure phase of NaAlH₄ is a monoclinic one (P2_{1/c} symmetry, fourfold coordination of the Al atoms, and designated as P2_{1/c}-4C-I) rather than the previously reported Cmc2₁ structure in Ref. 7.

However, we find the P2_{1/c}-4C-I phase is mechanically unstable and spontaneously transforms into another phase (named as P2_{1/c}-4C-II which also has the P2_{1/c} symmetry) with its lattice parameters of $a = 4.281 \text{ \AA}$, $b = 4.466 \text{ \AA}$, $c = 9.632 \text{ \AA}$, and $\beta = 92.9^\circ$. In the P2_{1/c}-4C-II phase, the Na and Al atoms occupy the 4e (0.221, 0.265, 0.241) and 4e (0.752, 0.193, 0.487) sites, and four nonidentical H atoms occupy the 4e (0.653, 0.319, 0.332), 4e (0.598, 0.827, 0.44),

4e (0.128, 0.545, 0.407), and 4e (0.936, 0.547, 0.103) sites. The P2_{1/c}-4C-II phase is energetically quite unfavorable within the whole pressure range. Thus, it should be excluded from the present discussion.

Structure searches for candidate high-pressure phases were performed by the *ab initio* evolutionary algorithm USPEX.^{12,13} This method has been used for many materials, including metal hydrides.¹⁴ All of the structures are optimized by the Vienna *ab initio* simulation package (VASP) code.¹⁵ We employ the generalized gradient approximation (GGA) with the Perdew-Wang (PW91) exchange-correlation functional and the projector-augment wave (PAW) method. A cutoff energy of 600 eV and a Monkhorst-Pack Brillouin zone sampling grid with the resolution of $2\pi \times 0.07 \text{ \AA}^{-1}$ were used. We performed structure prediction for NaAlH₄ at 0, 5, 10, 15, and 20 GPa with 6 and 12 atoms per unit cell. Phonon dispersion curves are calculated by the Quantum Espresso package.¹⁶ These calculations used the GGA-PW91 exchange-correlation functional, Vanderbilt ultrasoft potentials with a cutoff energy of 60 Ry for the wave functions, a $3 \times 3 \times 3$ and $3 \times 2 \times 3$ q -point meshes for the predicted P2_{1/c} and Ima2 phases, respectively. The powder x-ray diffraction (XRD) patterns are simulated using the REFLEX software.

Figure 1 displays four structures of NaAlH₄ at 15 GPa, including not only the reported I4_{1/a} and Cmc2₁ structures [Figs. 1(a) and 1(b)] but also the predicted P2_{1/c} and Ima2 structures [Figs. 1(c) and 1(d)]. Our calculated lattice constants of the I4_{1/a} and Cmc2₁ phases are in good agreement with the experimental and theoretical values.^{3,7} Although the theoretically predicted Cmc2₁ structure had been designated as the β phase,⁷ the recent experiment has proposed that the β phase has the P2_{1/c} symmetry. However, we find that the reported P2_{1/c}-4C-I structure is mechanically unstable.¹⁰ We predicted two thermodynamically stable alternative candidates that can resolve this problem. One structure is designated as P2_{1/c}-6C phase because it has P2_{1/c} symmetry with

^{a)}Electronic addresses: htwang@nankai.edu.cn and htwang@nju.edu.cn.

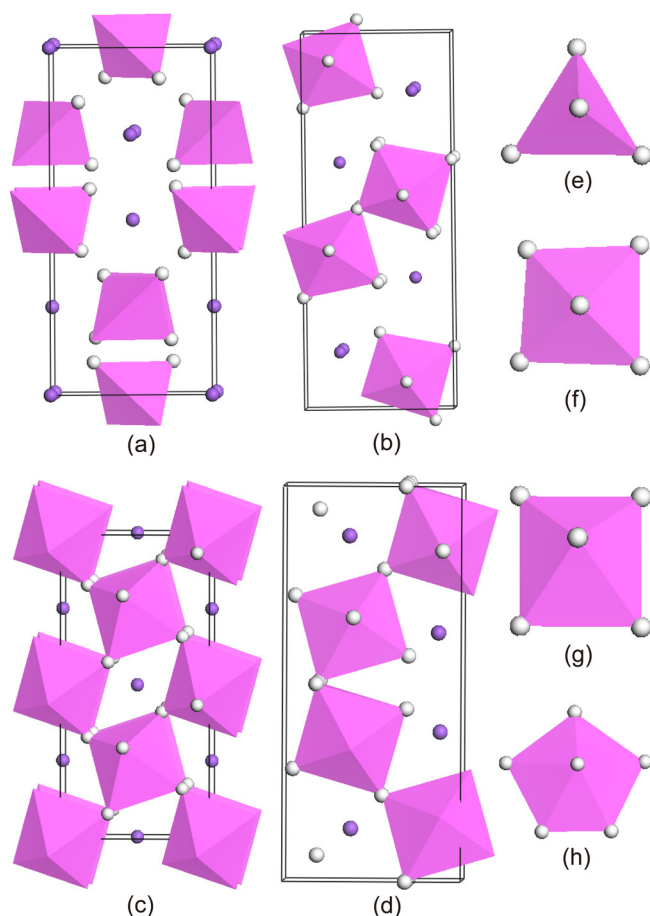


FIG. 1. (Color online) Crystal structures of (a) $I4_1/a$, (b) $Cmc2_1$, (c) $2 \times 1 \times 1$ supercell of $P2_1/c-6C$, and (d) $Ima2$ at 15 GPa. The pictures in (e), (f), (g), and (h) show the Na atoms and the complex anions for the $I4_1/a$, $Cmc2_1$, $P2_1/c-6C$, and $Ima2$ phases, respectively.

sixfold coordination of the Al atoms, in which Na atoms occupy the 2b (0.5, 0.0, 0.0) sites, Al atoms the 2c (0.0, 0.5, 0.0) sites, and two nonidentical H atoms the 4e (0.11, 0.666, 0.678), and 4e (0.321, 0.391, 0.071) sites at 15 GPa, respectively. The other is $Ima2$ phase, in which the Na atoms occupy the 4b (0.75, 0.627, 0.133) sites, Al atoms the 4b (0.75, 0.379, 0.64) sites, and four nonidentical H atoms the 4b (0.25, 0.335, 0.611), (0.75, 0.435, 0.311), (0.75, 0.217, 0.447), and 4a (0.0, 0.0, 0.312) sites (lattice constants are given in Table I).

As shown in Fig. 2, within the lower pressure range between 0 and 3.8 GPa, the most stable structure is the experimental one with the $I4_1/a$ symmetry. The $I4_1/a$ structure is then predicted by theory to transform into the $P2_1/c-6C$ structure at 3.8 GPa, a transition accompanied by a change from the AlH_4 -tetrahedral anion groups into the AlH_6 octahedral groups, as shown in Figs. 1(e) and 1(g). The $P2_1/c-6C$ phase is found to possess the lowest enthalpy over a wide pressure range from 3.8 to 20.5 GPa. In our earlier work, we found that the atomic charge distribution may serve as a criterion of stability at zero pressure.¹⁷ This is similar to the recently demonstrated correlation between the energy and geometric diversity of crystal structures (simpler structures are statistically more stable).¹⁸ Here, we have computed Bader charges,¹⁹ which turned out to be similar in the $P2_1/c-6C$, $Cmc2_1$ and $Ima2$ structures, $+0.76e$, $+0.75e$ and $+0.75e$

TABLE I. Calculated lattice constants and unit cell volumes V per formula unit at two different pressures ($P=0$ and 15 GPa), compared with other available data for the $NaAlH_4$ polymorphs.

Symmetry	P (GPa)	a (Å)	b (Å)	c (Å)	β (°)	V (Å ³)
$I4_1/a$	0	4.992	4.992	11.073		69.0
	15	4.497	4.497	9.576		48.4
$Cmc2_1$	0	4.997 ^a	4.997 ^a	11.083 ^a		69.2
	0	3.524	14.004	5.101		62.9
	15	3.374	11.850	4.726		47.3
$P2_1/c-6C$	0	3.549 ^a	13.830 ^a	5.113 ^a		62.8
	15	4.722	4.422	4.440	94.87	46.2
$P2_1/c-4C-II$	15	4.281	4.466	9.631	92.91	46.0
$P2_1/c-4C-I$	15	4.99 ^b	8.960 ^b	8.362 ^b	91.17	46.7
$Ima2$	15	3.779	10.061	4.523		43.0

^aReference 7.

^bReference 10.

for Na, $+2.26e$, $+2.26e$ and $+2.25e$ for Al, and $-0.79e$ ($-0.72e$), $-0.79e$ ($-0.71e$) and $-0.77e$ ($-0.71e$) for highest (lowest) charged H atoms, respectively. More homogeneous Bader charges in the $P2_1/c-6C$ phase correlate with its higher stability at zero pressure. Stability of the $Ima2$ phase at high pressure is then explained by its higher density and lower pressure-volume term in the Gibbs free energy. As the pressure increases, the $P2_1/c-6C$ phase undergoes a phase transition to the $Ima2$ structure, where the decahedral anions appear, as shown in Fig. 1(h). The transition pressure we predicted from $I4_1/a$ to $P2_1/c-6C$ is 3.8 GPa, which is much less than the experimental value of 14 GPa, even 6.4 GPa for the $Cmc2_1$ structure.^{7,8,10} The discrepancy in transition pressure between the theory and the experiment may be explained by the hysteresis in room-temperature compression and may also depend on the sample.^{7,9,10} Most strikingly, we find the transition pressure from $I4_1/a$ to $Ima2$ is 11.5 GPa, which is close to the measured value (~ 14 GPa).^{8,10} Moreover, the volume contraction of $Ima2$ at 15 GPa is 11% compared with 5% for $P2_1/c-6C$, which is in good agreement with the experimental value of 12%.¹⁰ Therefore, the coexistence of $P2_1/c-6C$ and $Ima2$ phases can explain better the experimental findings.

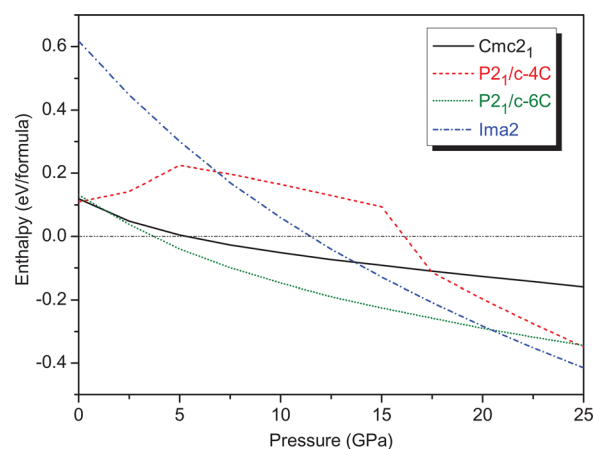


FIG. 2. (Color online) Dependence of the enthalpy (relative to the $I4_1/a$ structure) on the pressure, for the $Ima2$, $P2_1/c-4C-II$, $P2_1/c-6C$, and $Cmc2_1$ phases with respect to the $I4_1/a$ phase.

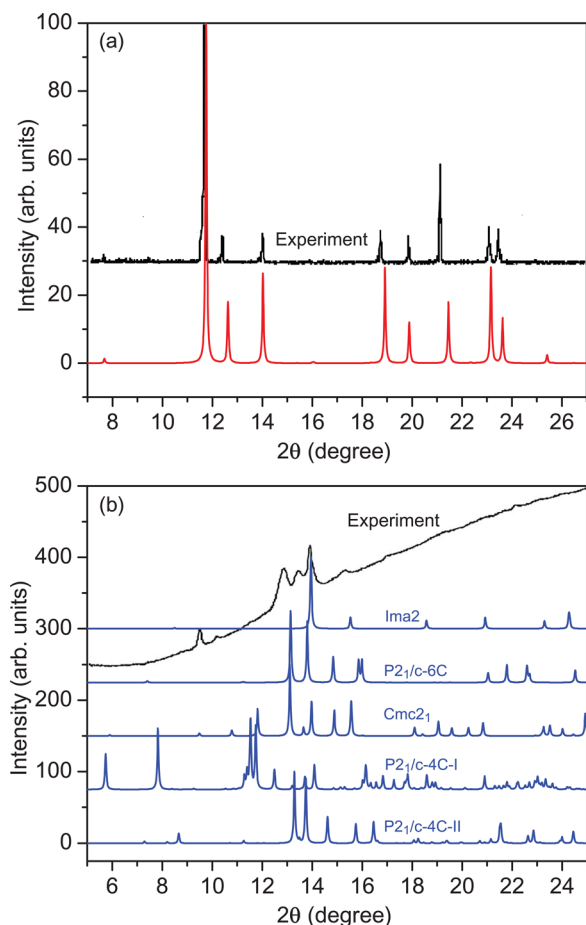


FIG. 3. (Color online) Simulated XRD patterns of (a) $I4_1/a$ at 0.6119 \AA compared with the experiment (Ref. 8) under ambient pressure and (b) $Ima2$, $P2_1/c-6C$, $Cmc2_1$, $P2_1/c-4C-I$, and $P2_1/c-4C-II$ structures at 15 GPa in comparison with the experimental result at 13.3 GPa.

To verify this idea, in Fig. 3(a), we show the simulated XRD pattern of the $I4_1/a$ phase at ambient pressure, which is identical to the experimental result.⁸ We also list the simulated XRD patterns of some related structures and the experimental data at 13.3 GPa.⁸ For the $P2_1/c-4C-I$ structure, as shown in Fig. 3(b), although the minor peaks at $2\theta \sim 14^\circ$ match very well with the observed data, the strongest peak located around 11.5° is away from the experimental value. In addition, there are other major peaks at 7.8° and 5.7° which are absent in the experimental data. For comparison, the strongest peaks of the $P2_1/c-6C$ and $Ima2$ phases are closer to the experiment than that of the $P2_1/c-4C-I$ phase. The common main peaks around 13° and 14° strongly overlap with those of $P2_1/c-6C$ and $Ima2$, which results in the spectral broadening in this region. The other peaks are relatively weak ($2\theta > 14^\circ$). Therefore, the simulated XRD pattern confirms that there may be coexistence of $P2_1/c-6C$ and $Ima2$ phases in experiment.⁸ We also note the discrepancy between the simulated and experimental spectrum around 9.5° . There are many possibilities: (1) other possible candidates for $NaAlH_4$ and (2) coexistence of many phases, such as intermediate high-pressure phase of Na_3AlH_6 or NaH . However, it is difficult to know the exact intermediate high-pressure phases or other corresponding crystal structures at present. The dynamical stability of the $P2_1/c-6C$ and $Ima2$ phases has been examined through the phonon calculations. The phonon dispersions of $P2_1/c-6C$ $NaAlH_4$ were calculated

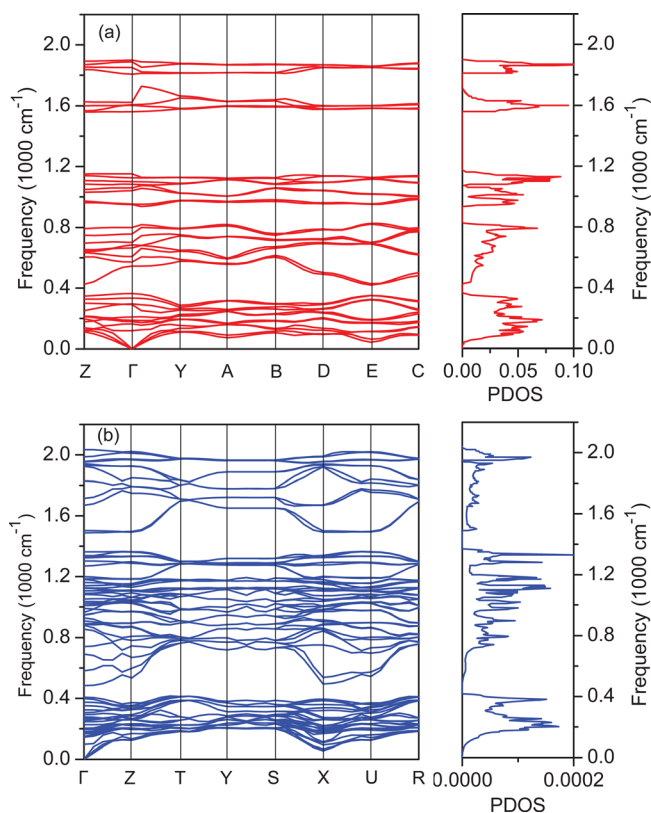


FIG. 4. (Color online) Phonon spectra and phonon density of states (PDOS) of (a) the $P2_1/c-6C$ phase at 10 GPa and (b) the $Ima2$ phase at 25 GPa.

from 5 to 20 GPa. The results indicate that the $P2_1/c-6C$ phase is dynamically stable at least in this pressure range as it has no imaginary phonon frequencies, as phonon dispersion at 10 GPa is shown in Fig. 4(a). However, the $P2_1/c-6C$ phase is unstable at 5 GPa due to the presence of imaginary frequencies, which is compatible with the measured Raman data (~ 4.6 GPa) during the decompression.¹⁰ As shown in Fig. 4(b), the $Ima2$ phase is dynamically stable at 25 GPa. Additional phonon calculations performed from 15 to 20 GPa reveal that the $Ima2$ phase can be stable at 20 GPa but has soft modes at 15 GPa, which indicates that the $Ima2$ phase is preserved only when the pressure exceeds 15 GPa, then reverts to the $P2_1/c-6C$ or $I4_1/a$ structures, which is also in agreement with the experimental findings.^{8,10}

In conclusion, we suggest that the coexistence of the $P2_1/c-6C$ and $Ima2$ phases can explain better the experimental findings.^{8,10} Charge disparity among H atoms correlates with structural stability. The $Ima2$ structure, in spite of being distorted and having Al atoms in the unusual sevenfold coordination, is much denser than other phases and becomes stable under pressure. This work provides the basis for the future investigations of possible explaining for the high-pressure phases in $NaAlH_4$.

This work was supported by the National Science Foundation of China (Grant Nos. 11174152 and 50821001), the 973 Program of China (Grant Nos. 2010CB731605 and 2011CB808205), the Postdoctoral Fund of China (Grant Nos. 20090460685 and 201104302), and the open project program of State Key Laboratory of Metastable Materials Science and Technology (Grant No. 201106). A.R.O. thanks Intel Corporation, Research Foundation of Stony Brook

University, Rosnauka (Russia, Contract 02.740.11.5102), DARPA (Grant N66001-10-1-4037), and National Science Foundation (EAR-1114313) for funding.

- ¹L. Schlapbach and A. Züttel, *Nature (London)* **414**, 353 (2001).
- ²J. Graetz, J. J. Reilly, J. Johnson, A. Y. Ignatov, and T. A. Tyson, *Appl. Phys. Lett.* **85**, 500 (2004).
- ³A. Peles and M. Y. Chou, *Phys. Rev. B* **73**, 184302 (2006).
- ⁴E. H. Majzoub, K. F. McCarty, and V. Ozolinš, *Phys. Rev. B* **71**, 024118 (2005).
- ⁵C. Moisés Araújo, R. Ahuja, J. M. Osorio Guillén, and P. Jena, *Appl. Phys. Lett.* **86**, 251913 (2005).
- ⁶B. C. Wood and N. Marzari, *Phys. Rev. Lett.* **103**, 185901 (2009).
- ⁷P. Vajeeston, P. Ravindran, R. Vidya, H. Fjellvåg, and A. Kjekshus, *Appl. Phys. Lett.* **82**, 2257 (2003).
- ⁸S. Nakano, A. Nakayama, and K. Takemura, in *Proceedings of the 20th AIRAPT Conference on High Pressure*, T10-P058 (2005).
- ⁹A. V. Talyzin and B. Sundqvist, *High Press. Res.* **26**, 165 (2006).
- ¹⁰R. S. Kumar, E. Kim, O. Tschauner, A. L. Cornelius, M. P. Sulic, and C. M. Jensen, *Phys. Rev. B* **75**, 174110 (2007).
- ¹¹R. S. Chellappa, D. Chandra, S. A. Gramsch, R. J. Hemley, J. F. Lin, and Y. Song, *J. Phys. Chem. B* **110**, 11088 (2006).
- ¹²A. R. Oganov and C. W. Glass, *J. Chem. Phys.* **124**, 244704 (2006).
- ¹³C. W. Glass, A. R. Oganov, and N. Hansen, *Comput. Phys. Commun.* **175**, 713 (2006).
- ¹⁴X. F. Zhou, A. R. Oganov, X. Dong, L. Zhang, Y. Tian, and H. T. Wang, *Phys. Rev. B* **84**, 054543 (2011).
- ¹⁵G. Kresse and J. Furthmüller, *Phys. Rev. B* **54**, 11169 (1996); *Comput. Mater. Sci.* **6**, 15 (1996).
- ¹⁶P. Giannozzi, S. Baroni, N. Bonini, M. Calandra, R. Car, C. Cavazzoni, D. Ceresoli, G. L. Chiarotti, M. Cococcioni, I. Dabo, *et al.*, *J. Phys. Condens. Matter* **21**, 395502 (2009).
- ¹⁷X. F. Zhou, Q. R. Qian, J. Zhou, B. Xu, Y. Tian, and H. T. Wang, *Phys. Rev. B* **79**, 212102 (2009).
- ¹⁸A. R. Oganov and M. Valle, *J. Chem. Phys.* **130**, 104504 (2009).
- ¹⁹W. Tang, E. Sanville, and G. Henkelman, *J. Phys. Condens. Matter* **21**, 084204 (2009).